

Scintillation Spectrometry of Low-Energy Bremsstrahlung*

Margarete Ehrlich

A method was devised to measure bremsstrahlung spectra from commercial X-ray tubes on an absolute scale, using a thallium-activated sodium-iodide crystal-scintillation spectrometer. The method was used to study bremsstrahlung spectra between 20- and 100-kilovolts exciting potentials from a beryllium window tube having a thick tungsten target. Fully corrected, absolute experimental spectra were obtained at exciting potentials of 50 and 100 kilovolts.

In order to compare the experimental results with theory, a calculation was made yielding the thick-target bremsstrahlung spectrum derived from Sommerfeld's theory. Experiment and theory showed order-of-magnitude agreement. However, a characteristic difference in spectral shape was observed, the experimental spectra showing a more pronounced peak. This peak is near 30 kilo electron volts and gives the impression of being superimposed on the spectral shapes expected from theory.

Finally, a point of interest to the practical user of the X-radiation from beryllium window tubes was brought out, namely, that a considerable portion of the low-energy radiation, at least in the region between 12 and 30 kilo electron volts, is strongly absorbed in the tungsten target of a conventional X-ray tube.

1. Introduction

1.1. Objective of the Present Study

Although high-energy bremsstrahlung spectra have recently been studied in great detail, a number of the more fundamental features of low-energy bremsstrahlung spectra, though under investigation for almost 40 years, have as yet not been satisfactorily explored. In fact, no absolute, fully corrected experimental data have ever been published, and no technique has been developed for a routine investigation of spectra from commercial X-ray tubes. It is the object of this paper to report on the design and performance of a scintillation spectrometer with a single thallium-activated sodium-iodide crystal that lends itself to the absolute determination of bremsstrahlung spectra from commercial X-ray tubes. So far, the instrument has been used up to 100-kv exciting potential only, but it is expected that with some modification of design it could be useful up to 150-kv and possibly to 200-kv exciting potential.

1.2. History of Bremsstrahlung Spectrometry

The history of the investigation of the nonrelativistic bremsstrahlung continuum is surveyed primarily by Kulenkampff [1, 2]¹ and by Finkelnburg [3].

a. Exploratory Experimental Work, Semiclassical Theory

The study of bremsstrahlung spectra received its first impetus from the experimental work of Laue and Bragg [4, 5], whose crystal diffraction spectrometer was until recently the only apparatus that lent itself to a satisfactory study of the bremsstrahlung

spectrum. The period between 1915 and 1930 produced the discovery and the experimental proof of the existence of a short wavelength limit of the bremsstrahlung continuum and of its dependence on electron velocity [6]. This period also produced the general exploratory studies of the spectral distribution as a function of electron energy and target material [7], the investigation of the efficiency of the process of bremsstrahlung production, and the first angular distribution studies that confirmed Sommerfeld's theoretical predictions [8, 9, 10].

In 1922, Kulenkampff measured the true spectral-intensity distribution of the bremsstrahlung from a number of different thick targets introduced into a gas-discharge tube that could be operated between 7 and 12 kv [11]. His measurements were fully corrected and absolute except for the conversion of the ionization in his detector (an air-ionization chamber) into units of absorbed photon energy. This conversion was not carried out because the wavelength dependence of the energy expended per ion pair was at the time unknown. Kulenkampff represented his corrected spectral-intensity data as a linear function of $(\nu_0 - \nu)$, where ν represents any bremsstrahlung frequency below ν_0 , the frequency at the Duane-Hunt limit. This expression is a very good approximation to his experimental spectral distributions.

Shortly thereafter Kramers published his semiclassical theory of the bremsstrahlung spectrum [12]. Kramers arrived at the frequency distribution of the total emitted radiation, starting with the classical expression for the spectral distribution of the energy radiated by an electron moving in the Coulomb field of an atomic nucleus. This yielded expressions for the bremsstrahlung intensity as a function of frequency. When these expressions are integrated over the target thickness, they take essentially the form of Kulenkampff's empirical thick-target formula.

*This article was composed for the fulfillment of the publication requirement for the degree of Ph. D. in the School of Arts and Sciences of the Catholic University of America, Washington, D. C.

¹ Figures in brackets indicate the literature references at the end of this paper.

Because of the considerable difficulties associated with exact experimental crystal spectrometry of the bremsstrahlung continuum, most of the experimental work confirming Kramers' theory was carried out by indirect methods. One of these, introduced by Webster and Hennings [13], consisted in isolating narrow spectral bands by means of suitable filtration and studying their intensity as a function of electron energy (Isochromatenmethode). From the partial information gained in this way, one can reconstruct the total spectral distribution. Another method, used for thin-target work by Duane [9], Kulenkampff [14], and Nicholas [15], and recently developed to a considerable extent by others [16, 17], consists in deducing the spectral distribution from the shape of absorption curves. Such an indirect method is probably adequate for the determination of heavily filtered or of unfiltered X-ray spectra close to the Duane-Hunt limit, but breaks down for the long-wave end of the spectrum. The reason for the use of indirect methods to supplement diffraction spectrometry becomes clear if one considers the optimum X-ray target design factors and the nature of the various distorting influences of the diffraction spectrometer: On the one hand, it is desirable to work with thin targets in order to minimize electron diffusion and energy loss through multiple non-radiative collisions in the target proper and to measure the bremsstrahlung spectrum produced by a truly monodirectional and monoenergetic electron beam. It is further desirable to have low-atomic-number targets in order to prevent the absorption of a portion of the bremsstrahlung by the target itself. On the other hand, because of the low efficiency of the diffraction spectrometer, it is important to produce high radiation fluxes—a requirement that called for target-design factors exactly opposite to those outlined before as optimum for the determination of an undistorted bremsstrahlung spectrum. Further complications are introduced by the fact that the reflectivity of the crystal varies with the wavelength of the incident radiation and that the factors entering into the determination of beam intensity from the measurement of ionization currents in air-ionization chambers are quite complex, and were at the time of the early bremsstrahlung studies not at all well understood.

b. Quantum-Mechanical Theory of the Nonrelativistic Bremsstrahlung Spectrum, Experimental Verifications

The impetus for this phase came clearly from the theoretical side. In 1929 and 1931, Sommerfeld published the results of his quantum-mechanical calculations. Limiting his calculations to non-relativistic velocities, to dipole transitions, and initially to unscreened fields, he arrived at an exact expression for the production of photons of given energy and direction by incident electrons of given energy [18, 19]. Finkelburg [2] points out that when integrated over all photon directions, Sommerfeld's expression for the X-ray spectrum shows a considerable formal similarity to that derived by

Kramers. It is, therefore, not too surprising that the spectral distributions measured by Kulenkampff and others show a fairly good qualitative agreement with both Kramers' and Sommerfeld's theoretical expressions. Later, Sommerfeld's theory was refined by Nedelesky, who introduced screening corrections in order to take account of the presence of the atomic electrons [20].

The progress in theoretical understanding of the problems of the nonrelativistic bremsstrahlung continuum was not matched by experimental advances, which could have facilitated thorough checks of the theory. The available experimental methods were still essentially the same as those used in the early studies. This fact may well be considered as one of the reasons why experimental work centered solely on studies of the angular distribution and polarization of the bremsstrahlung,² while no further attempts were made to measure absolute spectral intensities or to extend the studies of the spectral intensity distribution to higher electron energies. The only recent determinations of true spectra by direct methods seem to have been those by Kulenkampff and his coworkers [21, 22]. They used a hot-filament glass-bulb X-ray tube, with a massive tungsten target, and arrived at relative bremsstrahlung spectra obtained with exciting potentials up to 50 kv. After applying suitable corrections, they showed that their experimental data followed the empirical law found by Kulenkampff in 1922. They mention, however, that the conditions for targets of low atomic number seem to be more complex. Diffraction spectrometry was never attempted by direct methods on thin targets of low atomic number, probably in part because of the lack in efficiency of the old-type diffraction spectrometer and also because of the apparent shift in general interest in basic physics from low-energy atomic to high-energy nuclear physics; the latter may also have been one of the most important reasons for the fact that the curved-crystal spectrometer, which has proved so useful in gamma-line spectroscopy up to 1 Mev and higher [23], has never been used to study bremsstrahlung continua. However, the interest in the field seems to have been kept alive, if not for fundamental then at least for practical reasons, as shown by the renewed attempts to find indirect methods to arrive at spectral distributions of bremsstrahlung continua by way of absorption measurements [16, 17].

c. Scintillation Spectrometry

Around 1945 it became apparent that by coupling Rutherford's scintillating screen (first used for the detection of individual alpha particles) with a photomultiplier tube, one could produce an extremely sensitive system for the measurement of radiation energies and intensities [24]. Application of photomultiplier and electronic techniques, in conjunction with newly developed scintillator systems, eventually transformed this simple device into one of the most

² See the literature given in W. Finkelburg [3] and Kulenkampff's article [2].

powerful tools of modern physical research [25, 26, 27, 28]. In principle, the method is based on establishing simple relations between the readily measurable intensity of the light pulses within the particular scintillator and the energy of the incident photons (or particles), as well as between the number of lightpulses in the scintillator and the number of incident photons (or particles.)

Hofstadter was the first to use thallium-activated sodium iodide, NaI(Tl), for scintillation spectrometry and to show that this material is particularly suited for spectrometry of low-intensity photon sources [29, 30]. Subsequently, he and Johansson independently observed the "photolines" caused by the strong photoelectric absorption of monoenergetic photons in the iodine of the crystal [31, 32]. Hofstadter also established that the height of the light pulses ensuing from the impinging photons was proportional to the energy lost by the secondary electrons in the crystal [33]; also, that in a NaI(Tl) crystal large enough to facilitate total absorption of the radiation, the number of light pulses is equal to the number of impinging photons, which, in turn, is proportional to the total radiation flux [31, 33]. These facts established the usefulness of the NaI(Tl) scintillation counter—when coupled with a suitable pulse-height discriminator—for X- and gamma-ray spectrometry.

Up to now the scintillation spectrometer has been mainly used for gamma-line spectroscopy. However, in spite of its rather poor resolution (as compared with a diffraction spectrometer) the advantages of the scintillation spectrometer over the diffraction spectrometer for the measurement of continuous spectra are quite apparent. The diffraction spectrometer is complicated to operate, has a low yield that depends on photon energy in a complicated way, and is limited to comparatively low energies. No such inherent limitations exist for the NaI(Tl) scintillation spectrometer. It is of near-portable character, which makes its adaptation to a number of different problems of difficult geometries possible. Provided that the crystal is large enough to absorb the incident radiation in its entirety, its efficiency is equal to unity. At present, the high-energy limit of such a total-absorption spectrometer is given only by the maximum size of the available NaI(Tl) crystals. Its efficiency is so high that the problem is usually not how to obtain sufficiently strong radiation sources, but how to make them weak enough.

The first to use the NaI(Tl) scintillation spectrometer for a study of the bremsstrahlung spectrum was Johansson, who made a qualitative study of the spectrum from a commercial, thick-tungsten-target, glass-walled X-ray tube in the energy range from about 10 to 100 keV [34]. He corrected his experimental data for the change in instrument resolution with energy, but made no attempts to assess other distorting factors, such as absorption of the radiation in the tube window, the counter wall, or the intervening air. These corrections would be needed to allow a comparison of experiment and theory.

Subsequently, the NaI(Tl) scintillation spectrometer was used on several occasions for the measurement of "internal" bremsstrahlung, associated with the beta decay of a number of radioactive elements [35, 36]. In these studies the corrections for the change of resolution with energy were carried out in a manner similar to those applied in the case of magnetic spectrometry [37, 38, 39], and additional corrections for the escape of radiation energy in the form of iodine K fluorescence from the NaI(Tl) crystal surface were calculated [36]. Recently, Ramm and Stein [40] used a scintillation spectrometer to determine rough qualitative spectral distributions of heavily filtered X-ray beams from commercial tungsten target X-ray tubes, again without any further corrections or attempts of a comparison with the true, unfiltered bremsstrahlung spectrum. No other work on scintillation spectrometry of bremsstrahlung continua has so far been reported. However, it may be noteworthy that the use of a NaI(Tl) crystal counter as detector of the low-intensity X-radiation scattered off a quartz crystal enabled Beekman [40] to measure the spectrum of a commercial X-ray tube operated at 125 kv constant potential. Beekman's main interest lay in the determination of the influence of current waveform on spectral distribution, and he therefore made no effort to obtain absolute experimental data, to apply corrections, or to compare his results with theory.

2. The Experiment

2.1. Source of Bremsstrahlung

The most basic experimental study on bremsstrahlung would be that carried out on the spectra from a number of thin targets of different compositions. Work on 1-MeV thin-target spectra was recently performed at the National Bureau of Standards by Motz and Miller [42]. A thick-target X-ray tube was chosen for the present study, mainly because it was readily accessible and a study of its radiation could therefore be carried out with the expenditure of a minimum in funds, machine time, and personnel time. However, the theoretical problem presented by the radiation spectrum from such a thick-target tube is much more complicated than that from thin targets, and it can, in fact, not as yet be solved in great detail.

In order to facilitate a calculation of the absolute-intensity distribution emerging from the tungsten target proper, an experimental X-ray tube with a beryllium window of known thickness and approximately known purity was chosen for this study. The tube was held to constant potential with a ripple of less than 0.05 percent per milliampere. The potential across the tube was determined by means of measurements of the voltage drop across a calibrated 250-megohm resistor in series, and was maintained to an accuracy of less than 1 percent. Because of the high sensitivity of the spectrometer, it was necessary to operate the X-ray tube at extremely low currents. Such a procedure is justified under the assumption that a change in

tube current merely produces a change in X-ray intensity but not in spectral distribution. The tube currents were too low for conventional dynamical measurements, and for this reason the relation between tube current and the integral number of pulses counted in the detector system was established by the following indirect method: The tube was first operated on a relatively high current (order of magnitude of milliamperes) and a relation was established between tube current and ionization in a cavity chamber placed in the path of the radiation.³ The tube current was then lowered to fractions of a microampere (about $0.01 \mu\text{a}$) and the ionization in the cavity chamber was measured once more, this time simultaneously with the total number of pulses above a given height. The low-ionization measurements were carried out by a static method. The relation between tube current and total number of pulses above a given height was determined concurrently with the spectral measurement, which established the relation between the number of counts per minute per pulse-height interval and the total number of counts per minute above a given pulse height. The bias setting, which fixed the lower limit of pulse height for the total counts, was maintained constant to within 0.25 v throughout the entire experiment (which barely lasted more than 1 hour per spectrum).

2.2. Spectrometer Design Factors

It was essential to construct a crystal-photomultiplier assembly that would have good resolution, facilitate total absorption in the crystal, and have a window of considerable transparency to the incident radiation. A NaI(Tl) crystal lends itself especially well to this task in the low-energy region, because practically all photon absorption in the crystal takes place by photoelectric effect. In this case, the pulse-height distribution resulting from the absorption of monoenergetic photons consists of an essentially Gaussian curve, without any further disturbing distributions due to absorption by Compton effect or pair production. The broadening of monoenergetic lines into Gaussian distributions is mainly due to statistical fluctuations in pulse height originating at the emission from the cathode and the first few dynodes of the photomultiplier. Pulse-height resolution is customarily defined as a quantity proportional to the fractional mean-square deviation of pulse height for identical scintillations. Thus, as long as photon energy and pulse height are proportional, resolution should thus be inversely proportional to the square root of the photon energy.

A freshly-cleaved NaI(Tl) crystal, 0.5 in. high by 0.5 in. by 0.7 in., was chosen as the core of the detector. Calculation had shown that a crystal of these dimensions absorbs more than 99.99 percent of all incident radiation up to 80 keV in single photoelectric absorption events and about 98 percent

³ The ionization chamber had polystyrene walls, 0.001 in. thick, and although placed between the X-ray source and the spectrometer, its presence did not reduce the integral counting rate in the spectrometer, which was biased to record only pulses in the upper half of the spectrum.

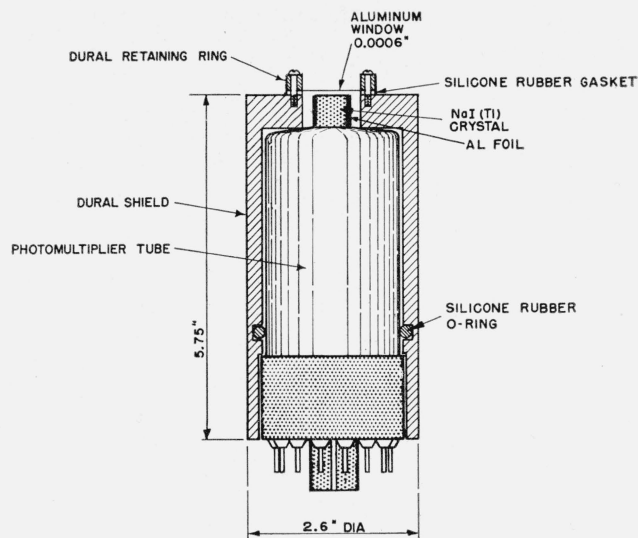


FIGURE 1. Photomultiplier—sodium iodide crystal assembly.

at 100 keV. The cube was sanded on the four side faces, which were then covered with aluminum foil for higher light-collecting efficiency. The upper and lower surfaces remained unsanded. The crystal was cemented to a Dumont K-1177 photomultiplier tube. The tube-crystal assembly was placed within an air-and-light-tight Dural can, filled with dry carbon dioxide of slightly higher than atmospheric pressure. Figure 1 shows the details of the assembly. The X-ray beam entered the assembly through an aluminum window, 0.0006 in. thick, after having been collimated by a 1-in.-thick brass diaphragm, of a diameter of approximately 6 MM. The diaphragm confined the radiation to the central portion of the crystal, without contributing any characteristic radiation within the measured energy range.

2.3. Experimental Setup

The essentials of the experimental setup are sketched in figure 2. The electrons impinged upon the target of the X-ray tube under an angle of 22 degrees, producing an X-ray beam whose central ray emerged from the X-ray tube in a direction perpendicular to the incident electrons. The X-ray beam, initially collimated by a 1-in. brass diaphragm close to the X-ray tube, reached the detector in a distance of 1 m from the target; the portion of the beam that entered the crystal subtended at the target a solid angle of 2.92×10^{-5} steradian. (The target dimensions were neglected in this estimate.) The electric pulses from the photomultiplier, corresponding to the light pulses in the NaI(Tl) crystal, were led through a cathode follower to a linear nonoverloading amplifier [43], giving pulses of a maximum height of 60 v, clipped by means of a delay-line to approximately square shape, and of about $10 \mu\text{sec}$ in duration. These pulses were monitored with an oscilloscope, and were also counted in a scaler (scaler I in figure 2). Simultaneously, the pulses were fed through a single-

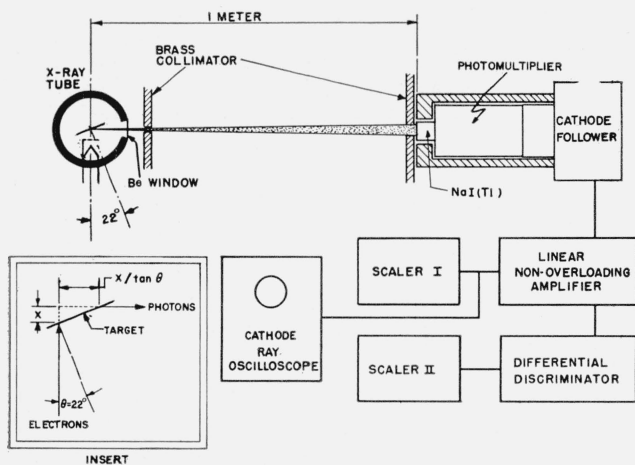


FIGURE 2. Details of the experimental setup.

Insert at lower left shows details of geometry of bremsstrahlung production.

channel differential pulse-height discriminator, and the number of pulses per channel width was determined by another scaler (scaler II in figure 2). Scaler II was biased to discriminate against low-noise pulses, and the bias on scaler I was adjusted so as to count only pulses above a certain height. This procedure allowed comparatively high differential counting rates in scaler II, at the same time keeping the integral counting rates in scaler I within reasonable limits. The differential counting rates varied between about 100 and 6,000 counts per minute; the integral counting rates did not exceed 3,500 counts per minute. In the case of the 50-kev and the 100-kev spectra, which were the only ones obtained on an absolute scale, the integral counting rates were used to tie in with the previously discussed current measurements.

2.4. Spectrometer Calibration

A calibration of resolution as a function of energy was obtained by determining the width of the pulse-height distributions at half height due to the K-fluorescence lines from nine different radiators. A radiator chamber similar to that described by Seemann [44] and a number of radiators supplied through the courtesy of Dr. Seemann were used for this purpose. The experimental setup is sketched in figure 3. Bremsstrahlung from a commercial tungsten-target X-ray tube operated at suitable voltages is made to impinge upon a sheet of the radiator material. The fluorescent radiation emerging under an angle of ninety degrees is analyzed in the NaI(Tl) crystal spectrometer. In order to isolate the fluorescence from high Z materials, suitably chosen filters have to be introduced in the path of the fluorescent radiation, in order to prevent the 90-degree Compton-scattered bremsstrahlung spectrum from being registered in the detector along with the K-fluorescence lines. No isolation of the K_{α} lines was attempted, as experiments had shown that, within the limit of the resolution of the instrument, the width of the K_{α} lines alone was the same as that

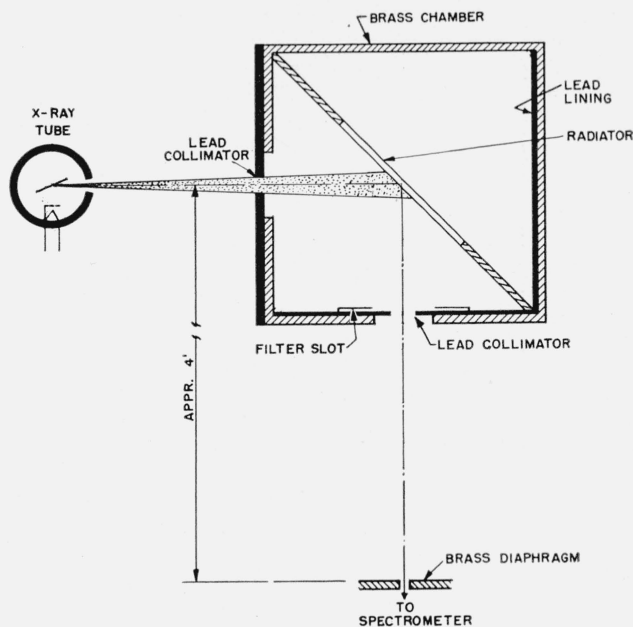


FIGURE 3. Fluorescence radiator chamber.

of the entire K series.⁴ Table 1 gives a list and description of the radiators used and of the filter materials that were found to be necessary to isolate the K-fluorescence lines, along with the exciting voltage for the bremsstrahlung used to produce the particular K fluorescence. Each pulse-height distribution was determined several times, each time with a different gain. The average resolution (in percent) was obtained for each line by computing the line width at half height in volts, expressed in percent of the pulse height at the fluorescence peak, also in volts.

TABLE 1. Fluorescence radiators and absorbers used to isolate fluorescence peaks

Radiator		Exciting bremsstrahlung potential	Absorber element and thickness
Element	$K_{\alpha 1}$ line		
	kev	kev	mm
Strontium.....	14.21	50	None.
Silver.....	22.23	50	Do.
Cadmium.....	23.24	50	Do.
Antimony.....	26.43	55 to 65	Do.
Lanthanum.....	33.53	55 to 65	Lead, 0.075.
Samarium.....	40.23	80	Lead, 0.075, plus gold, 0.050.
Tungsten.....	59.47	100	Silver, 0.57.
Gold.....	68.94	115	Lead, 0.95.
Lead.....	75.12	120 to 130	Do.

Samples of pulse-height distributions obtained for four of the fluorescent radiators were used to check the linearity of the energy scale, that is, the proportionality of the voltage at pulse-height maximum with the energy of the X-ray photons. Figure 4 shows the results of this check. The importance of the proper choice of filtration becomes apparent

⁴ This is not at all surprising, because the other lines of the K series are much less than one-half as intense as the K_{α} lines and can therefore not influence the K_{α} line width at half height.

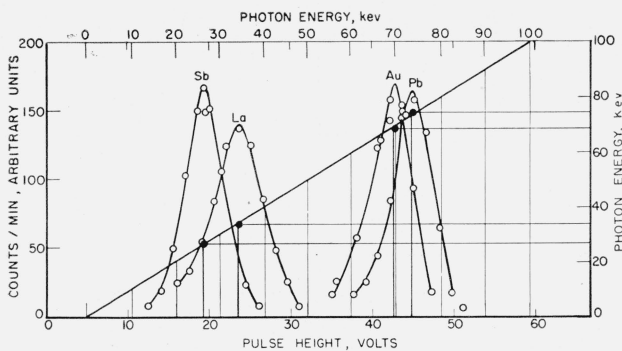


FIGURE 4. Energy-scale calibration of spectrometer.

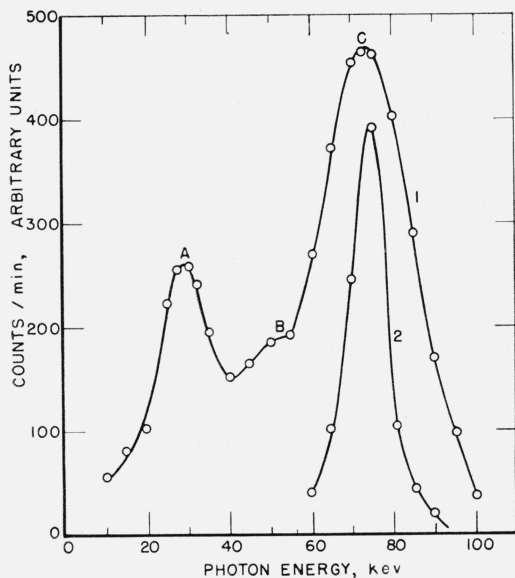


FIGURE 5. Pulse height distribution of fluorescence radiation from lead, irradiated with bremsstrahlung and observed perpendicular to the direction of bremsstrahlung incidence.

Curve 1. No filter between radiator and detector; A, peak of Compton-scattered bremsstrahlung spectrum; B, Compton-scattered K fluorescence peak from tungsten target; C, fluorescence peak from lead radiator.

Curve 2. 0.95 mm lead filter between radiator and detector.

in the pulse-height distribution shown in figure 4 for gold. This distribution was obtained with insufficient filtration and is therefore markedly skewed. The effect of filtration on the K-fluorescence pulse-height distributions is seen even better in the case of lead. Figure 5 shows the distribution obtained with a lead radiator, with and without filtration. When no filter is used, the entire bremsstrahlung spectrum, scattered through an angle of 90 degrees, is superposed on the lead K fluorescence. A 0.95-mm lead filter—although transparent to its own K fluorescence—strongly absorbs all lower energies, and thus isolates the lead K-fluorescence distribution. (The distribution below 60 keV, not shown in the graph, contained no points appreciably above background.)⁵

⁵ The resolutions shown for the lead-fluorescence pulse-height distributions, with and without added absorbers, are not quite comparable, as the two curves were obtained with different NaI(Tl) crystals.

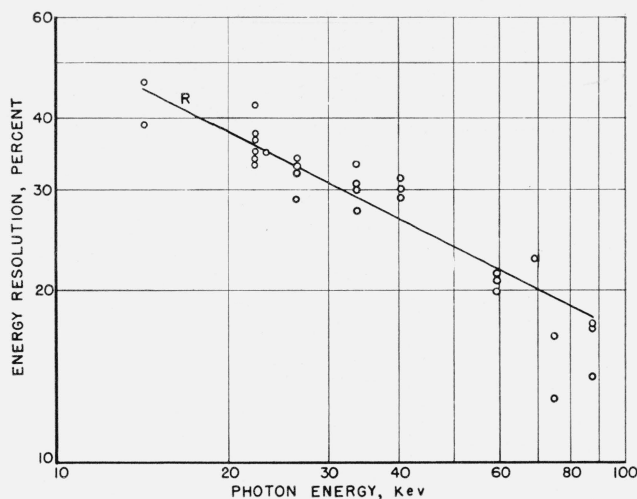


FIGURE 6. Percentage energy resolution of spectrum as a function of photon energy.

Figure 6 is a log-log plot of percentage resolution as a function of energy, obtained from the K-fluorescence data. Values obtained with the gamma rays from cadmium-109 and with the silver K fluorescence associated with the decay of cadmium-109 [45] are shown as well.

The line

$$R = \frac{168.0}{\sqrt{E}} + 0.1 \quad (1)$$

shown in the graph was fitted to the experimental data by the method of least squares. Equation (1) verifies the previously established fact that in this low-energy region the resolution depends primarily on the statistical distribution of the photoelectrons leaving the cathode of the photomultiplier. [46]

2.5. Raw Experimental Results

Figure 7 shows the differential counting rates obtained for the bremsstrahlung continua from the beryllium-window X-ray tube, operated at 50 and at 100 kv, as a function of photon energy. Due to the extremely low current levels used for this study, fluctuations in the bremsstrahlung intensity could not be entirely eliminated. For this reason, the quantity plotted on the ordinate is the following ratio:

$$\frac{C_{\text{diff}}}{C_{\text{total}}} \times \frac{C_{\text{total}}}{\text{ma}} \times \frac{1}{W} \quad (2)$$

C_{diff} is the differential counting rate per discriminator channel width; C_{total} , the integral counting rate; and W , the width of the discriminator channel, expressed in kilo electron volts. The plotted quantity is thus in units of number of differential counts per minute per milliamperere per kilo electron volt.

The two spectral distributions of figure 7 will be used in section 4 for an absolute comparison between theory and experiment. In order to give a better picture of how the spectral distributions change with exciting potential, five more spectra obtained at

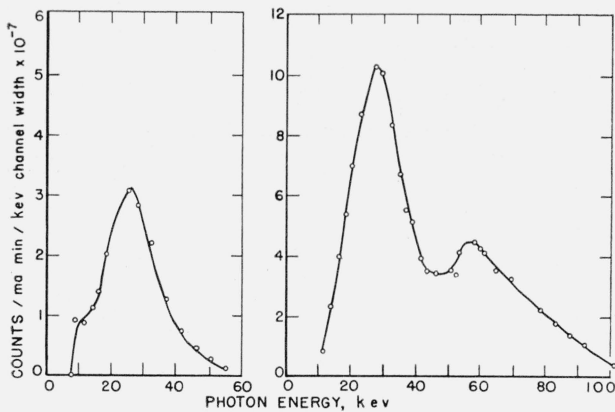


FIGURE 7. Differential counting rates, 50- and 100-keV bremsstrahlung spectra.

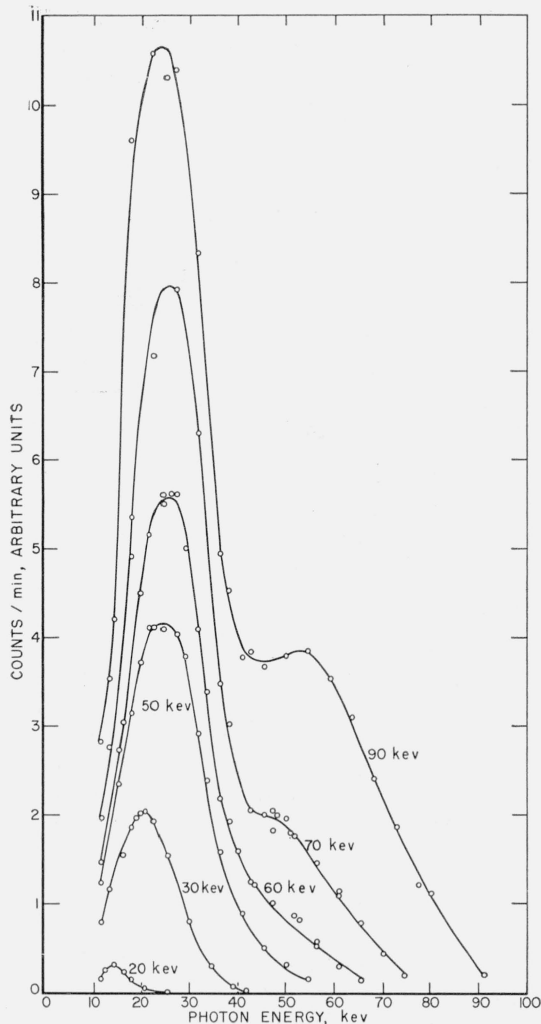


FIGURE 8. Change of spectral distribution with exciting potential.

exciting potentials between 20 and 100 kv are shown in figure 8. The ordinates of these spectra are not on a comparable scale.

The energy scales shown on the abscissas of figures 7 and 8 were obtained by a calibration of the spectrometer with the known gamma and X-ray lines of Cd^{109} . The differential counting rates are accurate to approximately ± 5 percent, the inaccuracy stemming from the limited counting statistics, as well as from the fluctuations in the discriminator channel width. There is an additional inaccuracy in the abscissa scale, amounting to about $\pm \frac{1}{2}$ volt in pulse height, due to limitations in the electronic stability of the system. The accuracy of the measurement of the current in the X-ray tube is estimated to be about ± 30 percent.

2.6. Correction of the Experimental Data

a. Variable Resolution

The problem of correcting the pulse-height distributions for variable finite resolution consists essentially in finding the relation between $C(E')$, the measured pulse-height distribution (number of counts per minute per discriminator window width)—corresponding to a particular measured photon energy interval between E' and $(E' + dE')$ —and $N(E)$, the true pulse-height distribution. It involves the solution of the following inhomogeneous Fredholm equation of the first kind:

$$C(E') = \int_0^{\infty} K(E, E') N(E) dE, \quad (3)$$

where $K(E, E')$, the kernel of the equation, represents a distortion function expressing the probability for a pulse due to photons of energy E to be recorded at the energy E' . Thus $K(E, E')$ is the function embodying the experimental data for the resolution of the detector as a function of energy.

In the energy region under consideration, the pulses of monoenergetic X- or gamma-ray lines were seen to be widened into Gaussian distributions of width $W(E)$ at half height due to the limited resolution. A valid representation of the distortion function K is therefore given by

$$K(E, E') = N e^{-(E-E')^2/2\sigma^2}, \quad (4)$$

where the mean-square deviation is given by $\sigma = [W(E)] / (2\sqrt{2\ln 2})$, and N represents the normalization factor. An equation of the type (3) lends itself readily to numerical evaluation with the aid of automatic computers. The method was first worked out by the Naval Research Laboratory group in connection with a somewhat different problem [47]. The method consists essentially in reducing the integral equation to an equation involving discrete sums. The function $K(E, E')$ becomes a matrix $(K_{E_i E_j})$ whose rank r (here chosen as 19) is equal to the number of selected discrete energy points, and the functions $N(E)$ and $C(E')$ become the r -dimen-

sional vectors (N_{E_i}) and (C_{E_j}) of the matrix equation

$$(C_{E'_j}) = (N_{E_i})(K_{E_i E'_j}) \Delta E_i. \quad (5)$$

Its solution for (N_{E_i}) , the true pulse-height distribution, is readily obtained by matrix inversion of $(K_{E_i E'_j})$ after the sum of the elements of each column of the matrix (K) has been normalized—a procedure taking the place of a normalization of the Gaussian function $K(E, E')$.

b. Crystal-Conversion Efficiency

Equation (3) actually contains another factor, namely, the efficiency of the spectrometer for the conversion of incident photons into electric pulses. As discussed earlier in this paper, at least 98 percent of all the impinging radiation are photoelectrically absorbed by the crystal. Furthermore, as no K-escape peaks [36] were ever observed on pulse-height distributions obtained with the particular spectrometer, it was concluded that the geometry of the detector was such that the escape of the iodine K fluorescence from the crystal surface was negligible. It was therefore considered legitimate to set the conversion-efficiency factor equal to 1.⁶

c. Absorption of Bremsstrahlung During Passage From Target to Detector

Table 2 lists the thicknesses and compositions of the absorbers in the path of the X-radiation and gives the values for the absorption corrections for 18 points between 10 and 100 keV. These values were computed with the aid of current absorption-coefficient tables [48]. The inaccuracies introduced in the absorption correction due to impurities in the

aluminum and beryllium were estimated to be less than 2 percent.

2.7. Corrected Experimental Spectra

The pulse-height distributions shown in figure 7 were corrected in the manner outlined in section 2.6. Figures 9 and 10 show the uncorrected distributions,

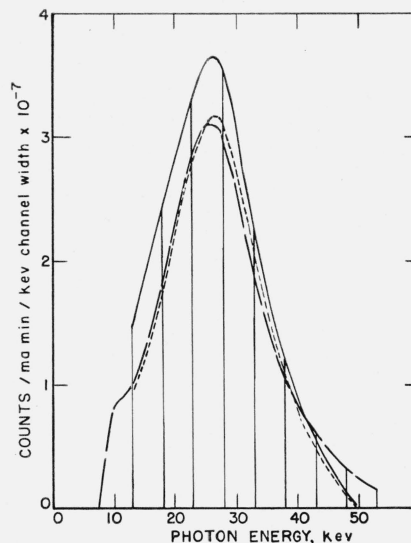


FIGURE 9. Correction of experimental data, 50-keV bremsstrahlung spectrum.

—, Uncorrected experimental data; — — —, experimental data corrected for finite spectrometer resolution; — · — ·, experimental data corrected also for absorption.

TABLE 2. Absorption of bremsstrahlung during passage from target to detector

Composition and thickness of absorbers			
Beryllium window, ^a 0.272 g/cm ² : 99.27% Be; 0.25% BeO; 0.10% Be ₂ C; 0.15% Al; 0.15% Fe; 0.08% Si.			
Aluminum window, 0.004267 g/cm ² : 99.5% Al; 0.1 to 1% Fe (considered as 0.5% in calculation); traces of Cu, Ni, Pb, Si, Ti, V, Zn, were neglected.			
Air, 0.1077 g/cm ² : 78% N ₂ ; 21% O ₂ ; 1% A.			
Total absorption correction as a function of quantum energy			
Quantum energy	Correction factor	Quantum energy	Correction factor
<i>kev</i>		<i>kev</i>	
13	1.52	58	1.06
18	1.29	63	1.06
23	1.19	68	1.06
28	1.12	73	1.05
33	1.09	78	1.05
38	1.08	83	1.05
43	1.07	88	1.05
48	1.07	93	1.05
53	1.05	98	1.05

^a The composition given for the beryllium window is that of the average stock of the Brush Beryllium Co., who furnished the window to the tube manufacturer.

⁶ Since this paper went to press, the spectrometer efficiency below 20 keV has decreased over the months. Some of the remarks below, about the lower portion of the spectrum, must accordingly be regarded with some caution.

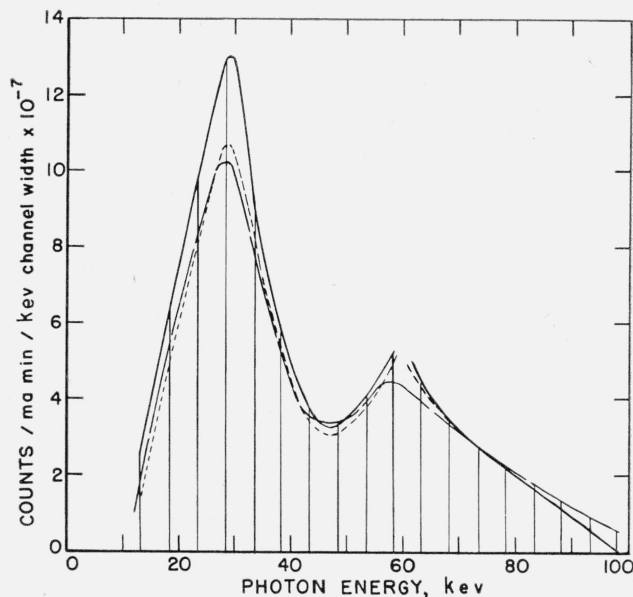


FIGURE 10. Correction of experimental data, 100-keV bremsstrahlung spectrum.

—, Uncorrected experimental data; — — —, experimental data corrected for finite spectrometer resolution; — · — ·, experimental data corrected also for absorption.

together with the distributions obtained in the energy interval between 13 and 100 keV after correcting for finite spectrometer resolution and after additional correction for absorption.

It is interesting to compare the spectra of figure 9, obtained with the beryllium-window tube, with the Compton-scattered-bremsstrahlung distribution of figure 5 from a tube with a window equivalent to $\frac{1}{2}$ -mm aluminum. The spectral peaks fall in both cases between 20 and 30 keV (note that the change in energy due to 90-degree Compton scattering of a 30-keV photon is negligible). Even after all the corrections for absorption in the materials between target and detector have been taken into consideration, the spectra from the beryllium-window tube still show a sharp intensity decline for energies below 25 to 30 keV. There is, furthermore, a quite distinct irregularity in the 50-keV spectrum near the tungsten L-absorption edge (see the uncorrected data) and only a comparatively small shift in the location of the ensuing spectral peak with an increase of the exciting energy from 50 to 100 keV. These facts make one suspect that the shape of the low-energy section of the spectrum is a property of the target rather than of the tube window.

The low-energy peak of the 100-keV spectrum is considerably more pronounced than that found by Johansson by scintillation spectrometry [34] or that found by Beekman by crystal spectrometry [41]. Experiments with two other NaI(Tl) detectors and an X-ray tube with higher inherent filtration confirmed that this difference is only in part due to the fact that an X-ray tube of lower inherent filtration was used for the present study. Also, it was found not to be a characteristic inherent in one particular NaI(Tl) detector.

The second, higher-energy peak appearing in the 100-keV spectrum and in all other spectra excited at potentials above 60 keV, is not a part of the bremsstrahlung, but represents the tungsten line spectrum ($K\alpha_1$ line at 59.5 keV). In spite of the corrections, this line spectrum—although approximately of the right over-all width—still appears entirely unresolved. This in part is probably due to the limited stability of the electronic equipment, and in part to the coarseness of the grid used in the discontinuous correcting procedure. The dotted line in figure 10 indicates the estimated course of the bremsstrahlung spectrum after the subtraction of the tungsten fluorescence peak and before correcting for absorption.

3. Theoretical Considerations

3.1. General Remarks

Kulenkampff, in his original experimental work on the thick-target bremsstrahlung spectrum [11], applied a number of corrections. These corrections stemmed in part from experimental and in part from theoretical considerations. He arrived in this way at a distribution for the bremsstrahlung spectrum from a thin target, and compared it with the then accepted theoretical expression.

For the present study, a slightly different approach was chosen. Because of the primary interest in the spectrum as it emerges from the target of a commercial X-ray tube, it was decided to apply the necessary corrections not to the experimental data but to Sommerfeld's expression for the cross section for thin-target bremsstrahlung. In this way, one arrives at an expression for the theoretical thick-target spectrum, and can compare it directly with the experimental spectrum emerging from the thick target (that is, after correcting the experimental data for absorption in air and in the other intervening materials). This procedure seems to be especially appropriate to this case, as only a rough estimate of the theoretical corrections has been made.

A precise calculation of the bremsstrahlung spectrum emerging from a massive target would require the following:

1. Integration of the thin-target spectrum over the path length of the electrons in the target, considering that, as the exciting electrons penetrate into the target, they soon lose their monoenergetic and monodirectional character due to nonradiative collisions within the target material. In consequence, the observed bremsstrahlung spectrum is not the one produced by a monodirectional, monoenergetic electron beam, as would be the case for a thin target, but is produced by a stream of electrons distributed in energy over a wide spectrum and having a complicated spatial distribution.

2. Correction of this spectrum for the losses in exciting electrons due to backscattering from the target.

3. Correction of this spectrum for the losses in emerging photons due to their absorption within the target material, taking into consideration the complicated spatial distribution of their origins, which is the result of the penetration and diffusion of the exciting electrons within the target. In spite of recent advances [49], the general theory of electron penetration and diffusion has not as yet progressed to a point where a detailed calculation of this type would be feasible. What can be done at the present time is, at best, in the nature of a rough estimate.

3.2. Present Approach

The present estimate followed the steps outlined in section 3.1. As some of the corrections are known only by order of magnitude, it was considered adequate to approximate the bremsstrahlung cross section by a simple analytical expression, and to carry out all integrations by graphical means. Following is a brief review of the procedure.

a. Bremsstrahlung Cross Section

According to theoretical considerations [50] electrons penetrating matter diffuse considerably before losing a substantial fraction of their energy. In fact, in a heavy element such as tungsten, they become practically completely isotropic before losing 10 percent of their initial energy.

It thus seemed reasonable to assume in this first

approximation that the bremsstrahlung was emitted by an isotropic distribution of electrons. Furthermore, even though the energy losses within the target are discontinuous, it is for the present purpose justified to carry out the integration as if the energy were a smooth function of path length. Then, if $i(E,k)dk$ is the nonrelativistic rate of bremsstrahlung emission per unit path length per unit solid angle, averaged over all directions, in the photon-energy interval between k and $k+dk$ (E being the exciting electron energy), the integral over the electron tracks in the target takes the form

$$I(E_0,k) = \int_{s=s_k}^0 i(E,k)ds = \int_{E=k}^{E_0} i(E,k)(ds/dE)dE, \quad (6)$$

where s is the depth of penetration, E is a function of s , and E_0 is the energy of the electrons before their penetration and diffusion into the target. For the actual calculations, values for $i(E,k)dk$ as obtained from the numerical computations of Kirkpatrick and Wiedmann [51] (which are based on the Sommerfeld formula) were used. They could be approximated by a function of the form

$$i(E,k) = \frac{1}{E} [a - b \ln(k/E)].$$

If $i(E,k)$ is in units of 10^{14} kev per steradian per milliampere per minute per unit kilo electron volt range per centimeter, and k and E are in kilo electron volts, the constant a is approximately equal to 16.7 and b is approximately 4.64. The reciprocal stopping power ds/dE was calculated with the aid of the Bethe-Bloch formula [52].

b. Correction for Backscattering of Electrons

The electron backscatter from the target was estimated, using Bothe's experimental results that give the probability $\beta'(E/E_0)d(E/E_0)$ for an electron of known initial energy E_0 and of known direction, to be backscattered with a known fraction E/E_0 of its primary energy [53]. For scattering materials of high atomic number and for a scattering angle of $50 \pm 15^\circ$, Bothe obtained for this probability a function that increases first slowly with increasing values of E/E_0 , then rises sharply to a maximum for E/E_0 somewhat above 0.9, and finally falls off to zero for $E/E_0=0.1$. A graphical integration of this function yields $\beta(E/E_0)$, the fraction of the total number of electrons, averaged over all angles, which is backscattered with energies between a given energy E and the maximum energy E_0 . According to Bothe, about 75 percent of the electrons incident on a block of tungsten are scattered back. This agrees very well with the observations of Seliger [54]. It was therefore decided to use for the present estimate Bothe's backscattering results by applying a correction term $1-\beta(E/E_0)$ to the integrand of eq (6). The equation then becomes

$$I'(E_0,k) = \int_k^{E_0} i(E,k)(ds/dE)[1-\beta(E/E_0)]dE. \quad (6a)$$

If $f_k(x)dx$ represents the fraction of the radiation of energy k produced at a depth x in the target measured in the direction of electron incidence, the fraction of the photons of energy k leaving the target is given by $\int_0^\infty f_k(x)dx \exp[-\mu(k)x/\tan \theta]$, where $x/\tan \theta$ represents the layer that the photons have to traverse when leaving the target, as seen by inspection of the insert in fig. 2. The integral can be written in the form $\exp[-\mu(k)\langle x \rangle_k/\tan \theta]$, where $\langle x \rangle_k$ is a suitable average of x over the function $f_k(x)$. Although this function is not well known, the average value $\langle x \rangle_k$ has been estimated, utilizing some general knowledge recently gained about the actual depth of electron penetration and bremsstrahlung production [49]. For the present approximate calculations, the value used for this average is one-fifth of the total electron range $p = \int_0^\infty (ds/dE) dE$, for all values of k .

The fully corrected spectrum was therefore represented by:

$$I''(E_0,k) = \exp[-\mu(k)p/5 \tan \theta] \int_k^{E_0} i(E,k)(ds/dE)[1-\beta(E/E_0)]dE. \quad (6b)$$

Essentially, this amounts to the assumption of $f_k(x) = \delta(x-p/5)$. This approximation is only adequate for $\mu(k)p \ll 1$. For $\mu(k)p \gg 1$ this exponential correction factor no longer holds, and the photon correction is approximated by $[f(0) \tan \theta]/\mu$.

For the present calculations, eq (6b) was used. The absorption-correction term was evaluated by setting the average depth of penetration ($p/5$) equal to 7.53×10^{-4} cm for 100-kev electrons and to 2.29×10^{-4} cm for 50-kev electrons. The total absorption coefficient for tungsten was obtained from current tables [48].

4. Comparison of Experiment and Theory

In order to facilitate a comparison between theory and experiment, the theoretical spectra corresponding to eq (6), (6a), and (6b) are shown in figures 11 and 12, along with the experimental photon-energy spectra. The experimental spectra were obtained from the fully corrected number-of-photons spectra of figures 9 and 10 by weighting the ordinates by the respective photon energies and dividing by 2.92×10^{-5} , which is the solid angle in steradians subtended by the spectrometer.

Considering the roughness of the theoretical estimate, the over-all order-of-magnitude agreement is quite good. There is, however, a remarkable difference in shape between the calculated and the measured spectra, the peak of the measured spectra in the neighborhood of 30 kev giving the impression of being superposed upon a continuous spectrum similar in shape to that of the calculated one. Figure 8 shows clearly how the 30-kev peak becomes

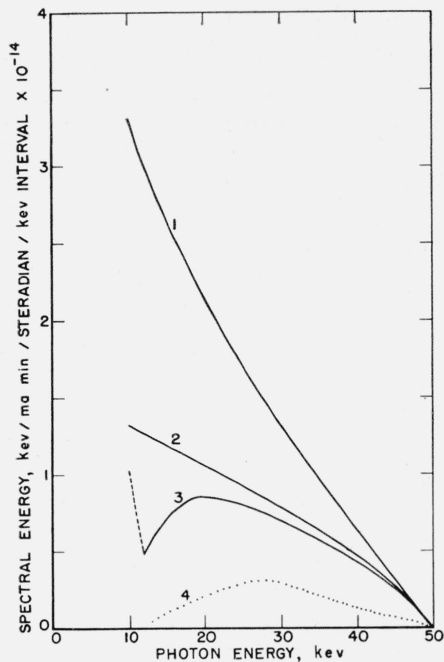


FIGURE 11. Comparison of experiment and theory, 50-keV bremsstrahlung.

1, No correction for electron backscatter or photon absorption; 2, theoretical thick-target spectrum corrected for electron backscatter; 3, theoretical thick-target spectrum, fully corrected; 4, experimental spectrum.

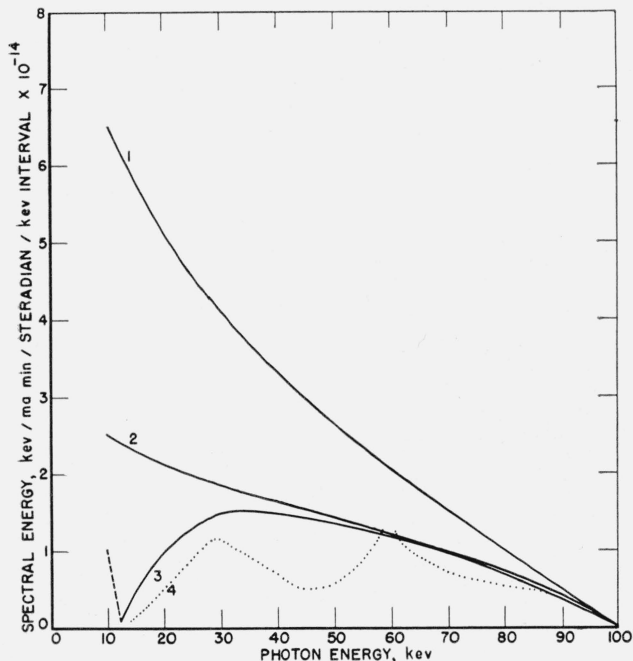


FIGURE 12. Comparison of experiment and theory, 100-keV bremsstrahlung.

1, No correction for electron backscatter or photon absorption; 2, theoretical thick-target spectrum corrected for electron backscatter; 3, theoretical thick-target spectrum, fully corrected; 4, experimental spectrum.

more and more intense as compared with the rest of the spectrum as the exciting potential is increased. As pointed out in section 2.7, the pronounced 30-keV peak was found with two different detectors and two X-ray tubes of different makes and inherent filtrations. Even if iodine K escape had not been found negligible with the detectors employed, the peak could not have been attributed to iodine K escape from the tungsten-fluorescence lines for two reasons: First of all, an approximate calculation of the iodine K escape expected from a 59.5-keV line would amount to only 4 percent of the total intensity of this line. The observed intensity increase above what is expected from theory, although at the right energy for the iodine K escape from the tungsten K-fluorescence lines, is too pronounced. Second, and quite convincingly, spectra determined experimentally behind varying thicknesses of different absorbers showed that a sufficient amount of filtration removed the spectral peak in the neighborhood of 30 keV almost completely, although it absorbed only a comparatively small fraction of the tungsten K fluorescence.

Another point of interest is the steep decrease of the experimental spectral intensity immediately below the 30-keV peak. An inspection of the theoretical curves of figures 11 and 12 shows that the absorption of the bremsstrahlung within the target is predominantly responsible for the peaks in the fully corrected theoretical distributions. This strengthens the suspicion that the shape of the low-energy portion of thick-target bremsstrahlung spectra is strongly influenced by the choice of the target material. Thus, in the case of a beryllium-window tube with a tungsten target, the effectiveness of the low-absorption window for passing low-energy X-radiation seems to be offset—at least above 12.12 keV, the energy of the tungsten L-absorption edge—by the strong absorption of these radiations within the tungsten target. The present measurements were not carried to low enough voltages to determine conclusively whether or not there is an appreciable rise in intensity below the L-absorption edge of tungsten.

The author is indebted to Professor L. F. Talbott of the Catholic University of America for his interest in the work, and to Evans Hayward of the National Bureau of Standards, whose vast experience was invaluable for the accomplishment of the experiment.

Thanks are also due to U. Fano, W. Miller, L. V. Spencer, and F. H. Day, all of the NBS Radiation Physics Laboratory, and to M. Newman of the NBS Computation Laboratory for their advice and assistance in the various phases of this work.

5. References

- [1] Handbuch der Physik **23**, 458 (Julius Springer, Berlin, 1926).
- [2] H. Kulenkampff, article in Physics of the Electron Shell, H. Kopfermann, editor, Fiat Review of German Science (1939-1946), Office of Military Government for Germany, Field Information Agencies Technical (1948).
- [3] W. Finkelburg, Kontinuierliche Spektren (Julius Springer, Berlin, 1938).
- [4] W. Friedrich, P. Knipping, and M. Laue, Ber. Bayer. Akad. Wiss. **303** (1912).
- [5] W. L. Bragg, Nature **90**, 410 (1912).
- [6] W. Duane and F. L. Hunt, Phys. Rev. **6**, 166 (1915).
- [7] C. T. Ulrey, Phys. Rev. **11**, 401 (1918).
- [8] H. Kulenkampff, Phys. Z. **30**, 450 (1928).
- [9] W. Duane, Proc. Nat. Acad. Sci. U. S. **13**, 662 (1927).
- [10] A. Sommerfeld, Phys. Z. **10**, 969 (1909).
- [11] H. Kulenkampff, Ann. Physik **69**, 548 (1922).
- [12] H. A. Kramers, Phil. Mag. **46**, 836 (1923).
- [13] D. L. Webster and A. E. Hennings, Phys. Rev. **21**, 312 (1923).
- [14] H. Kulenkampff, Ann. Physik **87**, 597 (1928).
- [15] W. W. Nicholas, BS J. Research **2**, 837 (1929) RP60.
- [16] J. R. Greening, Proc. Phys. Soc. (London) **63A**, 1227 (1950).
- [17] M. A. Greenfield, R. D. Specht, P. M. Kratz, and K. Hand, J. Opt. Soc. Am. **42**, 6 (1950).
- [18] A. Sommerfeld, Proc. Natl. Acad. Sci. U. S. **15**, 393 (1929).
- [19] A. Sommerfeld, Ann. Phys. **11**, 257 (1931).
- [20] L. Nedelsky, Phys. Rev. **42**, 641 (1932).
- [21] H. Kulenkampff and L. Schmidt, Ann. Physik **43**, 494 (1943).
- [22] R. Fuchs and H. Kulenkampff, Z. Physik **137**, 583 (1954).
- [23] J. W. M. DuMond, Rev. Sci. Instr. **18**, 626 (1947).
- [24] M. Blau and B. Dreyfus, Rev. Sci. Instr. **16**, 245 (1945).
- [25] I. Broser and H. Kallmann, Z. Naturforsch. **2a**, 439 (1947).
- [26] J. W. Coltman and F. Marshall, Phys. Rev. **72**, 528 (1947).
- [27] P. R. Bell, Phys. Rev. **73**, 1405 (1948).
- [28] Note also the comprehensive bibliography in A. T. Krebs, Scintillation Counters, Rep. No. 89, Radiobiology Dept., Army Medical Research Laboratory, Fort Knox, Ky. (1952); Medical Research and Development Board, Office of the Surgeon General, Department of the Army. Not published.
- [29] R. Hofstadter, Phys. Rev. **74**, 100 (1948).
- [30] R. Hofstadter, Phys. Rev. **75**, 796 (1948).
- [31] J. A. McIntyre and R. Hofstadter, Phys. Rev. **78**, 617 (1950).
- [32] S. A. E. Johansson, Nature **165**, 396 (1950).
- [33] R. Hofstadter and J. A. McIntyre, Phys. Rev. **79**, 389 (1950).
- [34] S. A. E. Johansson, Arkiv Fysik **3**, 533 (1951).
- [35] L. Madansky and F. Rasetti, Phys. Rev. **83**, 187 (1951).
- [36] T. B. Novey, Phys. Rev. **89**, 672 (1953).
- [37] G. E. Owen and H. Primakoff, Phys. Rev. **74**, 1406 (1948).
- [38] G. E. Owen and H. Primakoff, Rev. Sci. Instr. **21**, 447 (1950).
- [39] J. P. Palmer and L. J. Laslett, AECU-1220, Tech. Info. Serv., Oak Ridge, Tenn. (1951). Not published.
- [40] W. J. Ramm and M. N. Stein, Phys. Rev. **92**, 1081 (1953).
- [41] W. J. H. Beekman, Transactions, Instruments and Measurements Conference, Stockholm, p. 84-87 (1952).
- [42] J. W. Motz and William Miller, Phys. Rev. **96**, 544 (1954).
- [43] R. L. Chase and W. A. Higinbotham, Rev. Sci. Instr. **23**, 34 (1952).
- [44] H. E. Seemann, Rev. Sci. Instr. **21**, 314 (1950).
- [45] A. C. Helmholtz, Phys. Rev. **70**, 982, (1946).
- [46] A. W. Schardt and W. Bernstein, Rev. Sci. Instr. **22**, 1020 (1951).
- [47] L. A. Beach, R. B. Theus, and W. R. Faust, NRL Rep. 4277 (1953). Unpublished.
- [48] G. R. White, NBS Rep. 1003 (1952). Unpublished.
- [49] L. V. Spencer. To be published.
- [50] See, for instance, U. Fano, Radiation Biology, ch. 1, A. Hollaender, editor (McGraw-Hill, Book Co., Inc., New York, N. Y., 1954).
- [51] P. Kirkpatrick and L. Wiedmann, Phys. Rev. **67**, 321 (1945).
- [52] W. Heitler, The Quantum Theory of Radiation, p. 368, 3d ed. (Oxford Press, 1954).
- [53] W. Bothe, Z. Naturforsch. **4a**, 542 (1949).
- [54] H. H. Seliger, Phys. Rev. **78**, 491 (1950).

WASHINGTON, November 22, 1954.